Supplemental Material

Timing between successive introduction events determines establishment success in bacteria with an Allee effect.

Supplemental Methods

Determining the effect of storing the engineered bacteria temporarily at 4ºC

To determine if bacterial density changes significantly when bacteria were held at 4 ºC during our multiple introduction experiment, we prepared and diluted bacteria as described in "Multiple introductions experiment (main text)" without IPTG in the medium. We placed the bacteria at 4ºC, and measured CFUs after 0 hrs, 12 hrs, and 24 hrs of storage time as previously described (1). We then compared the density between the time points using a two-tailed t-test. A minimum of three biological replicates were used for analysis.

Determining growth rate

An overnight culture was diluted 1000-fold into 200 μL of fresh M9 medium (without IPTG) that was contained in the well of a 96-well plate (Genesee Scientific). The media in the microplate was overlaid with 70 μL of mineral oil, and placed in a Victor X4 microplate reader that was preheated to 37ºC. Every 10 min, the plate was shaken with a radius of 0.1 mm for 10 seconds on the fast setting, and OD_{600} was measured. Growth was determined by fitting a linear line through the region of the growth curve where there was a linear increase in growth. The slopes of these linear lines ($R^2 \geq 0.99$) were then compared using a two-tailed t-test. Three biological replicates were performed.

Estimating the magnitude of τ

To determine the amount of time required for bacteria to grow (required to estimate the magnitude of τ), bacteria were diluted 20-fold in M9 medium with IPTG and various percentages of casamino acids. The diluted bacteria were then grown, and OD_{600} was measured, as described in "Determining growth rate." τ was then estimated as described below in "Parameter estimation." A minimum of three biological replicates were used for analysis.

Determining the Allee threshold in M9 medium with different percentages of casamino acids

To determine if changing the percentage of casamino acids in the growth medium changed the Allee threshold, bacteria of various initial densities (as performed in figure 1c) were inoculated into medium (with IPTG) containing different percentages of casamino acids. After 24 hrs, the change in CFUs and OD_{600} was quantified. A statistical analysis was performed to determine if changing the percentage of casamino acids significantly influenced the Allee threshold. To accomplish this, initial densities were binned based on average growth dynamics observed when measuring CFUs (a lack of or consistent decrease in CFU, a decrease to no change in CFU, a consistent increase in CFU, bin ranges reported in figure S4). A two-tailed t-test was used to compare between the binned ranges to examine if there was a difference in the change in CFUs (figure S4d) and OD_{600} (figure S4e).

Model development

The mathematical model (Eq. 1 and 2, main text) is from a previously published manuscript from the senior author. For a full derivation of the model, including alternative formulations (using stochastic differential equations, assuming leaky expression of AHL, basal

death rate) that lead to qualitatively similar results observed in a previous manuscript, please consult (1).

To simulate experiments where two introductions of bacteria were performed, we initialized the simulation using a given initial density, C, of bacteria. After time δ, which represents the time of the second introduction, we added in a second density, C, of bacteria. These bacteria were added to the total amount of bacteria remaining at time δ. For simplicity, we did not account for the additional medium/nutrients that was added at the second introduction event as the volume of medium is relatively small (max 19 μL) relative to the total volume of medium in the well (500 μL). It is unlikely that a small increase in nutrients at time δ can account for the dynamics that we observed in our experimental system. For the majority of the simulations, we used a value of t = 150 hrs so that the system reaches steady state.

Parameter estimation

The values of parameters used in our model are located in Table S3. We estimated μ from growth curves of bacteria grown in the absence of IPTG (1). We estimated the value of k_{dA} from previously published literature (2). Note that a previous publication has observed that AHL degrades according to first order kinetics (3). We estimated the value of k_A from previously published literature (4, 5).

We estimated the order of magnitudes of γ and β by considering the length of the *ccdB-lacZα* and *ccdA* genes and proteins, transcription (6) and translation rates (7) in exponentially growing *E. coli*, the folding time for the proteins (~10-20 s), the estimated molecular weight of the CcdB-LacZα (~ 21 kDa) and CcdA (~8 kDa) proteins and the volume of a bacterial cell (~ 4 x 10^{-15} L) (8). Using this data, we estimated that γ and β should have orders of

magnitude of 0.001 μM/hr and 0.001 μM, respectively. We then fit the values of these parameters to our experimental data. A more detailed description and derivation of γ and β can be found elsewhere (1).

To estimate τ, we estimated the time point at which bacteria stopped growing due to inhibition by CcdB (figure S3, region indicated with solid arrows, experiment performed as described above). We then estimated the time point at which bacteria began growing again due to AHL and rescue via CcdA (figure S3, region indicated with dotted arrows). The time between these two time points represents the total time required to synthesize, and use, AHL for growth. We estimated the value of this time and divided it in half to account for additional molecular interactions that lead to relief from CcdB including synthesis of CcdA, the time required to CcdA to bind to and inhibit CcdB, and the time for cells to recover from CcdB poisoning (9).

To estimate the range of C in our experiments, we determined the carrying capacity of M9 medium containing IPTG (3.12×10^7 CFU/mL +/- 2.82×10^7). We then estimated the value of C which would represent ~10^4 CFU/mL (Allee threshold), which was on the order of magnitude of 0.001.

We note that the estimated values of these parameters are in line with two of our previous publications that have used the same bacteria under similar growth conditions (1, 10).

Simulations using coupled gene expression and growth

Previous studies have indicated that increasing growth rate will increase the number of proteins per cell (11). In our system, increasing growth rate could increase γ, β, and k_A. To simulate the effect of coupling gene expression to growth rate, we simulated two scenarios:

the effect of increasing γ, β, and k_A with increasing growth rate, and the effect of increasing just k_A with increasing growth rate. We assumed that the expression of all three would increase identically as both are driven by very similar promoters (P_{lac} vs. $P_{lac/ara}$) and are induced using IPTG. Based on a previous publication, we assumed that doubling the growth rate would increase the amount of protein by approximately 25% (11). We scaled the interactions between γ, β, and k_A, and μ using this approximation.

Supplemental Results

Simulation results using coupled gene expression and growth

Simulations using coupled gene expression and growth produced the same qualitative trends as uncoupled gene expression and growth (figure S6d). With uncoupled growth, as μ is decreased, the values of δ that lead to growth contract. Eventually, growth is not observed for all values of δ if μ is sufficiently small. When the value of k_A was coupled to μ, our model predicts that the values of δ that lead to growth decreases faster with decreasing μ and that the bacteria will fail to grow at higher values of μ (figure S6d, bottom panel). As compared to the simulation with uncoupled gene expression and growth (figure S6d, top panel), the curve maintains its same general shape but shifts to the right. When the values of γ, β, and k_A were coupled to μ, our model predicts that the values of δ that lead to growth decreases slower with decreasing μ and that the bacteria will fail to grow at lower values of μ (figure S6d, bottom panel). As compared to the simulation with uncoupled gene expression and growth, the curve shifts slightly to the left but maintains its general shape.

Supplemental Figure Legends:

Figure S1: Diagram of gene circuit conferring the Allee effect to our engineered bacteria. An IPTG inducible P_{lac} promoter regulates expression of the toxin protein CcdB, which kills the cell by inhibiting gyrase (12). The *luxR*/*luxI* quorum sensing system is activated by IPTG via the $P_{lac/ara}$ promoter. The LuxI protein produces an acylhomoserine lactone (3OC6HSL, AHL), which can be shared amongst all members of the bacterial population. Once AHL has reached a sufficiently high concentration, it binds to the LuxR protein, and drives expression of the *ccdA* gene (regulated by the P_{lux} promoter). The CcdA antitoxin protein prevents cell death, and allows growth, by interfering with the CcdB toxin protein (13). Construction and additional testing of circuit functionality can be found in (1).

Figure S2: Temporarily storing the engineered bacteria at 4°C does not decrease cell density. We serially diluted bacteria near the Allee threshold in M9 medium (without IPTG), and stored the bacteria at 4°C. CFUs were measured upon serial dilution (time = 0 hrs), and after 12 and 24 hrs. $P > 0.5$ when the 0 hr measurement is compared to 12 and 24 hr measurements (two-tailed t-test). Standard deviation from a minimum of three replicates. This indicates that in our multiple introductions experiment, large changes in CFUs in the second introduction event cannot account for the growth dynamics observed.

Figure S3: Growth dynamics of bacteria with Allee effect circuit activated. OD_{600} initially increased but was then stalled after approximately ~400 min (~ 6 hrs, indicated by solid arrow), which indicates the time point at which CcdB inhibits cell growth. To estimate τ, we identified the region where growth resumed due to the accumulation of AHL (indicated by

dotted arrow). τ was then estimated as described in Supplemental Methods. Standard deviation from a minimum of three biological replicates.

Figure S4: The effect of changing the percentage of casamino acids in M9 medium on the Allee threshold.

a) Growth rate of the bacteria in M9 medium (no IPTG) with different percentages of casamino acids. Standard deviation from a minimum of three biological replicates. Comparison between 0.1% and 1%, $P < 0.01$. Comparison between 0.1% and 2%, $P < 0.001$. Comparison between 1% and 2%, $P < 0.01$ (two-tailed t-tests).

b) Change in CFUs of bacteria grown in medium for 24 hrs with different percentages of casamino acids (with IPTG). Final CFU did not increase, on average, if initial CFU was below 10^4 CFU/mL. Statistical analysis showing that the Allee threshold does not change with the percentage of casamino acids in M9 medium in figure S4d. For panels b-e, 0.1% = light blue, 2% = dark blue.

c) OD_{600} at 24 hrs of bacteria grown as in panel b. OD_{600} did not increase at or below the Allee threshold ($P > 0.17$ when $\sim 10^4$ is compared to zero, both growth media, one-tailed t-test).

d) The change in CFU over 24 hrs for engineered bacteria grown in medium with different percentages of casamino acids. To determine if the Allee threshold changed, we binned the initial densities at, near, and above the Allee threshold. P values (two-tailed t-test) > 0.35 for all comparisons between media for each binned initial density range. This indicates that the growth trends, as measured using CFU, were the same between each binned range. Binned initial density ranges (CFU/mL) $<10^3 = 2.5 \times 10^-$

^{2} – 3.7 x 10^{3}, ~10^{4} (Allee threshold) = 4.2 x 10^{3} - 5.3 x 10^{4}, >10^{5} = 1.1 x 10^{5} – 6.0 x 10^{6} CFU/mL.

e) OD_{600} at 24 hrs of engineered bacteria grown as in panel b. Using similar binned ranges as above (panel d), we compared OD_{600} between binned initial densities from bacteria grown in the different media. While the binned density encompassing the highest initial densities was different (owing likely to growth rate, $P < 0.001$, two-tailed t-test), the binned densities encompassing the Allee threshold and below were not different ($P > 0.34$, two tailed t-test). This indicates that the growth trends, as measured using OD_{600}, were the same between the two lowest binned ranges. Binned initial densities: <10^{3} = 1.4 x 10^{2} – 3.55 x 10^{3}, ~10^{4} (Allee threshold) = 4.2 x 10^{3} - 5.3 x 10^{4}, >10^{5} = 1.85 x 10^{5} – 3.9 x 10^{7} CFU/mL.

Figure S5: Control experiments and simulations for our multiple introduction experiments.

a) OD_{600} of bacterial populations after two introduction events of the same cell density (two 10 μL introduction volumes), and either without IPTG in the medium (red circles, 4.28 x 10^{4} CFU/mL +/- 8.02 x 10^{4}) or above the Allee threshold (with IPTG, blue circles, 4.91 x 10^{5} CFU/mL +/- 4.13 x 10^{5}). Standard deviation from a minimum of three biological replicates. OD_{600} at 36 hrs. Green shaded region indicates growth (one-tailed t-test, Table S4). Zero hr data point (no second introduction) shown as a control.

b) Simulations using our mathematical model (Eq. 1-2, main text) showing the change in bacterial density (C) as a function of initial C. With the circuit OFF ($\gamma = 0$), C increases regardless of initial C (except for when initial $C \geq 1$, carrying capacity and above). With the circuit ON ($\gamma = 0.0048$), growth occurs if initial C is sufficiently high. t = 36 hrs.

Model development and parameter estimation in Supplemental Methods, and Table S3.

Figure S6: Sensitivity analysis and control simulations when manipulating the growth rate of the bacteria.

a) Simulations showing the effect of changing μ on value of A at t = 24 hrs. Initial C = 0.003. γ = 0. No second introduction.

b) Simulations showing the effect of one initial introduction event (C = 0.003, circuit ON). Without the second introduction event, regardless of μ, growth does not occur. For panels b, c, d and e, t = 150 hrs. For b and c, value of μ indicated in panel.

c) Simulations showing the effect of inactivating the circuit (γ = 0, and C = 0.003 for both introduction events). Growth occurs (C increases) at all values of μ and δ.

d) Simulations showing how coupling gene expression (k_A, β, and γ) with growth (μ) affects the values of δ that lead to an increase in C. Top panel: Simulation using uncoupled growth replotted from figure 3b as a comparison. Bottom panel: Coupling between k_A, and μ plotted in the bright purple line. Coupling between k_A, β, and γ, and μ plotted in the dark purple line.

e) Simulations showing how changing the values of parameters k_A, k_{dA} and τ affect the relationship between μ and δ. Values used for simulations throughout the manuscript indicated with *. Changing the values of k_A, k_{dA} and τ serves to shift the region that allows for growth (increase in C) to higher or lower values of μ. The qualitative shape of the curves is generally maintained except for when τ is very small (0.1).

Figure S7: Simulations showing how changing the values of parameters k_A, k_{dA} and τ affects the greatest value of δ that leads to growth (increase in C). Values used for simulations throughout the manuscript shown in the center panels. Changing the values of k_A, k_{dA} and τ serves to shift the region that allows for growth to higher or lower values of initial and second C. The qualitative shape of the landscape plot is generally maintained.

Figure S8: Control simulations using different values of C for the first and second introduction events.

a) Simulation showing the effect of one initial introduction event (circuit ON, $\gamma = 0.0048$). Without the second introduction event, regardless of C, growth does not occur. Initial C indicated on plot. In both panels, lines are stacked on top of each other. For both panels, $t = 150$ hrs.

b) Simulations showing the effect of inactivating the circuit ($\gamma = 0$). Growth occurs (increase in C) at all values of C and δ. Total $C = 0.006$.

Figure S9: Simulations showing the dynamics of C and A when varying the density of C introduced in the first and second introduction events. The value of initial C is indicated along the left hand side of the plots. Green shading indicates growth (increase in C) at $t = 150$ hrs. Total C for each simulation = 0.006. The value of δ is indicated along the top of each column. The same axes scales are used for C and A in each plot.

Supplementary Literature Cited

1. Smith R, Tan CM, Srimani JK, Pai A, Riccione KA, Song H, et al. Programmed Allee effect in bacteria causes a tradeoff between population spread and survival. Proc Natl Acad Sci USA. 2014;111(5):1969-74.

2. Kaufmann GF, Sartorio R, Lee S-H, Rogers CJ, Meijler MM, Moss JA, et al. Revisiting quorum sensing: Discovery of additional chemical and biological functions for 3-oxo-N-acylhomoserine lactones. Proc Natl Acad Sci USA. 2005;102(2):309-14.

3. Wang YJ, Leadbetter JR. Rapid acyl-homoserine lactone quorum signal biodegradation in diverse soils. Appl Environ Microb. 2005;71(3):1291-9.

4. Pai A, You L. Optimal tuning of bacterial sensing potential. Mol Syst Biol. 2009;5:286.

5. Ravn L, Christensen AB, Molin Sr, Givskov M, Gram L. Methods for detecting acylated homoserine lactones produced by Gram-negative bacteria and their application in studies of AHL-production kinetics. J Microbiol Methods. 2001;44(3):239-51.

6. Vogel U, Jensen KF. The RNA chain elongation rate in Escherichia coli depends on the growth rate. J Bacteriol. 1994;176(10):2807-13.

7. Dennis PP, Bremer H. Differential rate of ribosomal protein synthesis in Escherichia coli B/r. J Mol Biol. 1974;84(3):407-22.

8. Volkmer B, Heinemann M. Condition-Dependent Cell Volume and Concentration of Escherichia coli to Facilitate Data Conversion for Systems Biology Modeling. PLoS ONE. 2011;6(7):e23126.

9. Dwyer DJ, Kohanski MA, Hayete B, Collins JJ. Gyrase inhibitors induce an oxidative damage cellular death pathway in Escherichia coli. Mol Syst Biol. 2007;3.

10. Wilson C, Lopatkin A, Craddock T, Eldakar O, Driscoll W, Lopez J, et al. Cooperation and competition shape ecological resistance during periodic spatial disturbance of engineered bacteria. Sci Rep. 2017;7(440).

11. Klumpp S, Zhang Z, Hwa T. Growth rate-dependent global effects on gene expression in bacteria. Cell. 2009;139(7):1366-75.

12. Dao-Thi M-H, Van Melderen L, De Genst E, Afif H, Buts L, Wyns L, et al. Molecular basis of gyrase poisoning by the addiction toxin CcdB. J Mol Biol. 2005;348(5):1091-102.

13. Afif H, Allali N, Couturier M, Van Melderen L. The ratio between CcdA and CcdB modulates the transcriptional repression of the ccd poison–antidote system. Mol Microbiol. 2001;41(1):73-82.

14. Eschtruth AK, Battles JJ. Assessing the relative importance of disturbance, herbivory, diversity, and propagule pressure in exotic plant invasion. Ecol Monogr. 2009;79(2):265-80.

15. Gertzen EL, Leung B, Yan ND. Propagule pressure, Allee effects and the probability of establishment of an invasive species (Bythotrephes longimanus). Ecosphere. 2011;2(3).

16. Brockerhoff EG, Kimberley M, Liebhold AM, Haack RA, Cavey JF. Predicting how altering propagule pressure changes establishment rates of biological invaders across species pools. Ecology. 2014;95(3):594-601.

17. Wittmann MJ, Metzler D, Gabriel W, Jeschke JM. Decomposing propagule pressure: the effects of propagule size and propagule frequency on invasion success. Oikos. 2014;123(4):441-50.

18. Drake JM, Baggenstos P, Lodge DM. Propagule pressure and persistence in experimental populations. Biol Lett. 2005;1(4):480-3.

19. Blackburn TM, Prowse TAA, Lockwood JL, Cassey P. Passerine introductions to New Zealand support a positive effect of propagule pressure on establishment success. Biodivers Conserv. 2011;20(10):2189-99.

20. Moulton MP, Cropper WP, Avery ML. Historical records of passerine introductions to New Zealand fail to support the propagule pressure hypothesis. Biodivers Conserv. 2012;21(1):297-307.

21. Nunez MA, Moretti A, Simberloff D. Propagule pressure hypothesis not supported by an 80-year experiment on woody species invasion. Oikos. 2011;120(9):1311-6.

22. Barney JN, Ho MW, Atwater DZ. Propagule pressure cannot always overcome biotic resistance: the role of density-dependent establishment in four invasive species. Weed Res. 2016;56(3):208-18.

23. Ketola T, Saarinen K, Lindstrom L. Propagule pressure increase and phylogenetic diversity decrease community's susceptibility to invasion. BMC Ecol. 2017;17.

24. Sagata K, Lester PJ. Behavioural plasticity associated with propagule size, resources, and the invasion success of the Argentine ant Linepithema humile. J Appl Ecol. 2009;46(1):19-27.

25. Britton JR, Gozlan RE. How many founders for a biological invasion? Predicting introduction outcomes from propagule pressure. Ecology. 2013;94(11):2558-66.

26. Clark GF, Johnston EL. Propagule pressure and disturbance interact to overcome biotic resistance of marine invertebrate communities. Oikos. 2009;118(11):1679-86.

27. Warren RJ, Bahn V, Bradford MA. The interaction between propagule pressure, habitat suitability and density-dependent reproduction in species invasion. Oikos. 2012;121(6):874-81.

28. Hedge LH, O'Connor WA, Johnston EL. Manipulating the intrinsic parameters of propagule pressure: implications for bio-invasion. Ecosphere. 2012;3(6):1-13.

29. Ahlroth P, Alatalo RV, Holopainen A, Kumpulainen T, Suhonen J. Founder population size and number of source populations enhance colonization success in waterstriders. Oecologia. 2003;137(4):617-20.

30. Simkanin C, Davidson IC, Therriault TW, Jamieson G, Dower JF. Manipulating propagule pressure to test the invasibility of subtidal marine habitats. Biol invasions. 2017;19(5):1565-75.

31. Koontz MJ, Oldfather MF, Melbourne BA, Hufbauer RA. Parsing propagule pressure: Number, not size, of introductions drives colonization success in a novel environment. Ecol Evol. 2018;8(16):8043-54.

32. Sinclair JS, Arnott SE. Relative importance of colonist quantity, quality, and arrival frequency to the extinction of two zooplankton species. Oecologia. 2017;184(2):441-52.

33. Sinclair JS, Arnott SE. Strength in size not numbers: propagule size more important than number in sexually reproducing populations. Biol Invasions. 2016;18(2):497-505.

34. Vahsen ML, Shea K, Hovis CL, Teller BJ, Hufbauer RA. Prior adaptation, diversity, and introduction frequency mediate the positive relationship between propagule pressure and the initial success of founding populations. Biol Invasions. 2018:1-9.

Supplemental Tables:

Table S1. Examples of studies linking, or not linking, propagule pressure to establishment success.

	Main Finding	Reference
Propagule pressure promotes establishment success	Canopy disturbance and propagule pressure of exotic plant invasion are most important predictors of *Alliaria petiolata*, *Berveris thunbergii*, and *Microstegium vimineum* establishment and invasion.	(14)
	A positive correlation exists between propagule pressure and probability of *Bythotrephes longimanus* establishment.	(15)
	There is a positive correlation between interception frequency (surrogate of propagule pressure) and establishment for *Scolytinae* and *Cerambycidae* species.	(16)
	Using an ecological modelling approach, the product of propagule size and frequency correlate more strongly with invasion success than either single component alone.	(17)
	Increasing propagule pressure increased establishment in *Daphnia magna*.	(18)
	Propagule pressure is positively related to establishment success from re-analysis of New Zealand bird introduction data.	(19)
Propagule pressure does not promote establishment success	Initial releases of New Zealand bird species explain establishment success as opposed to introduction frequency and high introduction number	(20)
	Three estimates of propagule pressure (number of introduced individuals, number of areas introduced, and number of years during which species was planted) for 130 species of woody plants did not predict successful establishment and invasion.	(21)
	Propagule pressure does not determine invasion success for communities with high invasion resistance, particularly for species *Urochloa platyphylla, Digitaria sanguinalis, Abutilon theophrasti,* and *Amaranthus* retroflexus, which experience strong density-dependent inhibition.	(22)
	Using *Pseudomonas chlororaphis, Pseudomonas putida,* and *Escherichia coli,* establishment and invasion success does not depend only on propagule pressure.	(23)
	Propagule pressure did not influence establishment for *Linepithema humile* in field studies.	(24)

Table S2. The effect of propagule size and number on establishment success from select experimental studies.

Component of Propagule Pressure	Effect on Establishment Success	Finding	Reference
Propagule size	Positive	Increasing the propagule size of the invasive fish *Pseudorasbora parva* increased establishment success.	(25)
		Increasing propagule size of *Watersipora subtorquata* increased establishment success in disturbed and undisturbed environments.	(26)
		Increasing the propagule size *Microstegium vimineum* seeds can reduce the inhibitory effects of an unsuitable growth environment, which could enhance establishment success.	(27)
		Increasing propagule size increased the establishment success of *Crassostrea gigas*.	(28)
		Large propagule size and a high number of source populations increased colonization probability of *Aquarius najas*.	(29)
		Increasing the propagule size of *Botrylloides violaceus* larvae increased the number of individuals that became established	(30)
	Negative	Changing propagule size did not have a significant effect on establishment success of *Daphnia magna*. Immigration rate (propagule size x propagule number) was more important in determining establishment.	(18)
Propagule number	Positive	Increasing the propagule number increased the number of individual *C. gigas* that successfully colonized, and increased the long term survival of the population.	(28)
		Increasing propagule number increased the probability of establishment of *T. castaneum* in simulated microcosm experiments.	(31)
		Increasing propagule number of *Skistodiaptomus oregonensis* increased the percentage of populations that became established.	(32)
	Negative	Increasing the propagule number of *Hemimysis anomala* decreased population persistence.	(33)
		Increasing propagule number of *Tribolium castaneum* increased the mortality of founding individuals.	(34)
	No effect	The timing between introduction events had no effect on the establishment of *T. castaneum* populations	(34)
		Changing propagule number did not have a significant effect on establishment success of *D. magna*.	(18)
		Propagule number did not have an apparent influence on establishment success of *P. parva*. However, only one propagule size (above the threshold required for establishment) was examined.	(25)

Table S3. Baseline parameters used in our model (Eq. 1 and 2).

Parameter	Description	Value	Reference
β	Half maximal killing ability of CcdB	0.007 μM	Estimated as described above
γ	Killing rate of CcdB	0.0048 μM/hr	
k_{sA}	Synthesis rate of AHL	0.25 μM/hr	(4, 5)
k_{dA}	Degradation rate of AHL	0.15 /hr	(2)
μ	Maximum growth rate	0.5 /hr	(1)
τ	Time delay of the activation of gene expression by the LuxR-AHL complex	7 hrs	Estimated as described above (figure S3)
δ	Time between the first and second introduction events	0.001 - 50 hrs.	

Table S4. A summary of P-values obtained in our multiple introduction experiments. P values were determined using a one-tailed t-test and compared against zero. Significance level was determined using a Benjamini-Hochberg procedure. Bolded P values indicate that OD_{600} values for that condition were not statistically different than zero (i.e., no growth).

IPTG	Percentage of Casamino Acids	Introduction Volumes (µL)		0 hr	Time to second introduction										figure
					2 hr	4 hr	6 hr	8 hr	10 hr	12 hr	14 hr	16 hr	20 hr	24 hr	
NO	2 %	10	10	< 0.001	< 0.001	< 0.001	< 0.001	< 0.001	< 0.001	< 0.001	< 0.001	< 0.001	< 0.001	< 0.001	S5a
YES				< 0.001	0.025	-	**0.037***	0.016	0.028	0.002	-	-	**-**	0.001	
				1	0.008	< 0.001	< 0.001	< 0.001	< 0.001	< 0.001	< 0.001	0.013	**1**	**0.211**	2a, 3a, 4a
		15	5	**1**	0.019	< 0.001	< 0.001	< 0.001	0.008	< 0.001	0.011	0.014	0.001	**0.101**	4a
		19	1	**1**	0.020	0.002	0.004	0.003	0.008	0.001	0.004	0.023	0.006	0.028	
		5	15	**1**	0.010	< 0.001	< 0.001	< 0.001	< 0.001	< 0.001	< 0.001	0.002	< 0.001	**0.088**	
		1	19	**1**	< 0.001	< 0.001	< 0.001	< 0.001	< 0.001	< 0.001	0.007	0.002	0.002	0.003	
	1 %	10	10	**1**	-	**1**	**1**	**1**	0.003	0.004	0.008	**0.172**	**0.165**	**0.081**	3a
	0.1 %			**1**	-	**1**	**1**	-	**1**	**1**	**1**	**1**	**1**	**1**	

* this P value was above the significance value of 0.035 as determined using the Benjamini-Hochberg procedure. However, this is likely a type II error because all OD_{600} values associated with this P value are significantly above zero (0.281, 0.416 and 0.138)

figure S1

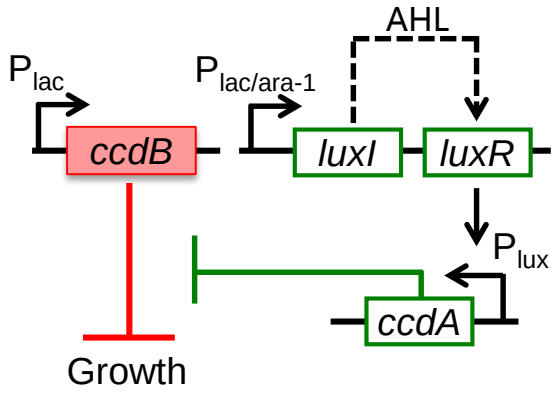

figure S2

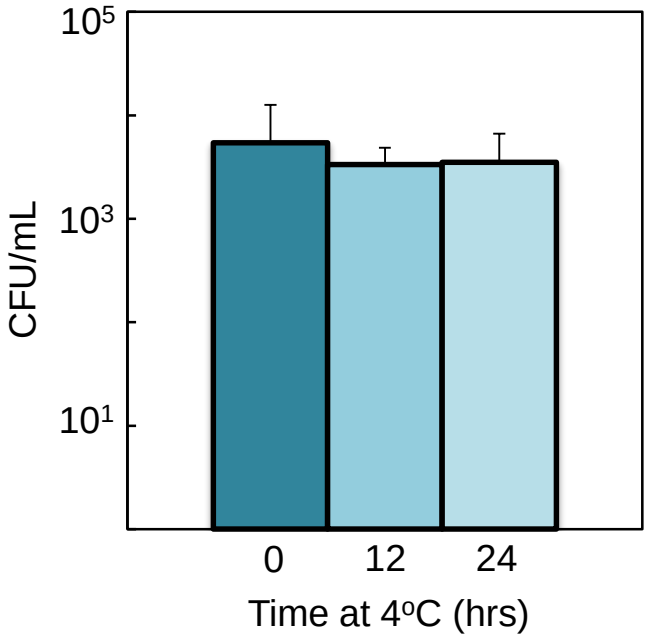

figure S3

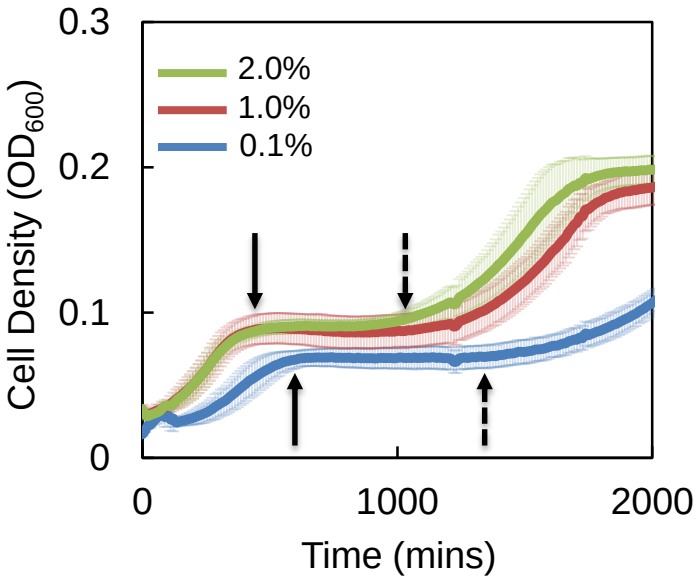

figure S4

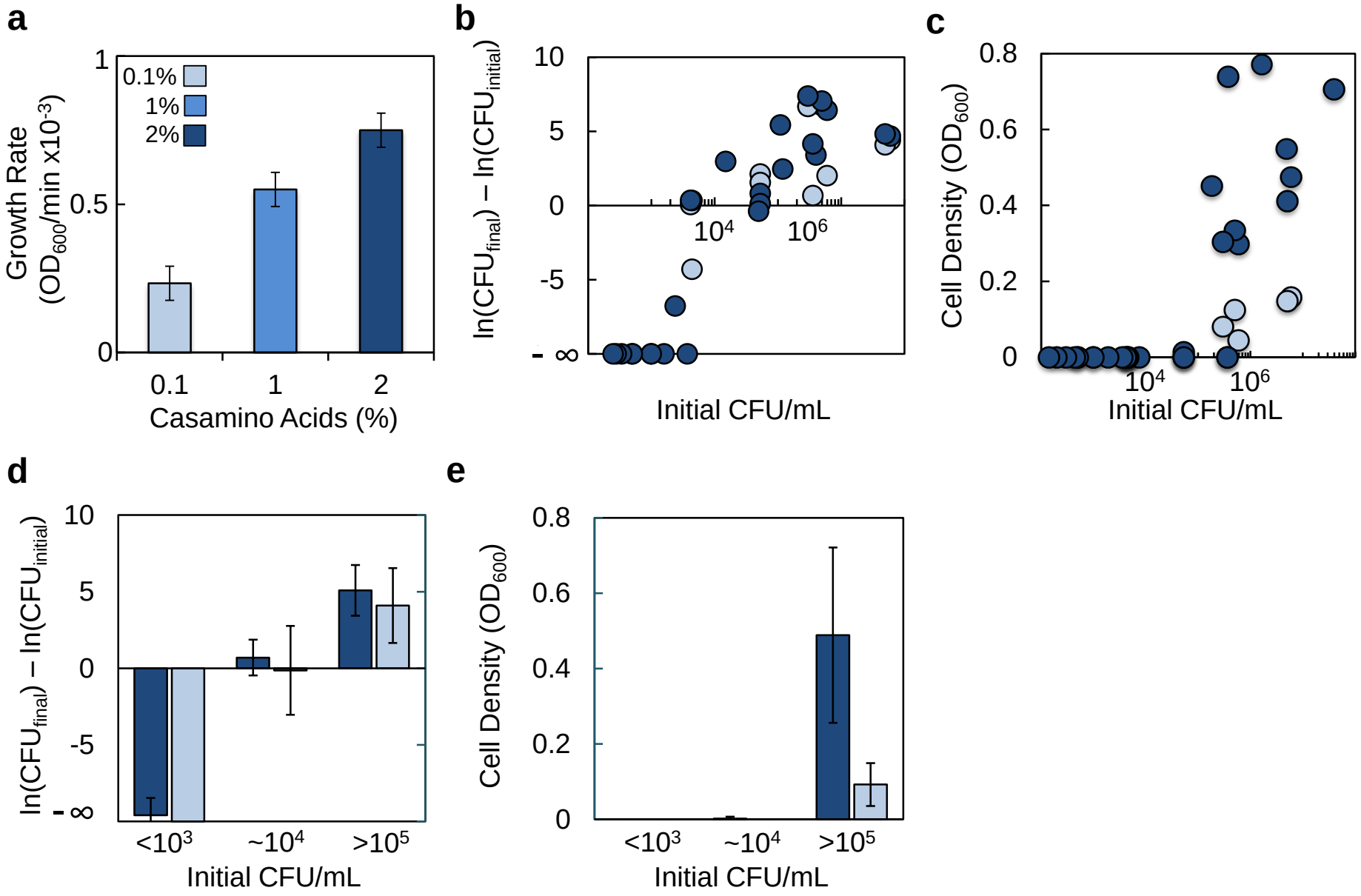
a
Growth Rate
(OD600/min x10-3)
1
0.5
0
0.1%
1%
2%
0.1
1
2
Casamino Acids (%)
b
ln(CFUfinal) – ln(CFUinitial)
10
5
0
-5
- ∞
10^4
10^6
Initial CFU/mL
c
Cell Density (OD600)
0.8
0.6
0.4
0.2
0
10^4
10^6
Initial CFU/mL
d
ln(CFUfinal) – ln(CFUinitial)
10
5
0
-5
- ∞
<10^3
~10^4
>10^5
Initial CFU/mL
e
Cell Density (OD600)
0.8
0.6
0.4
0.2
0
<10^3
~10^4
>10^5
Initial CFU/mL

figure S5

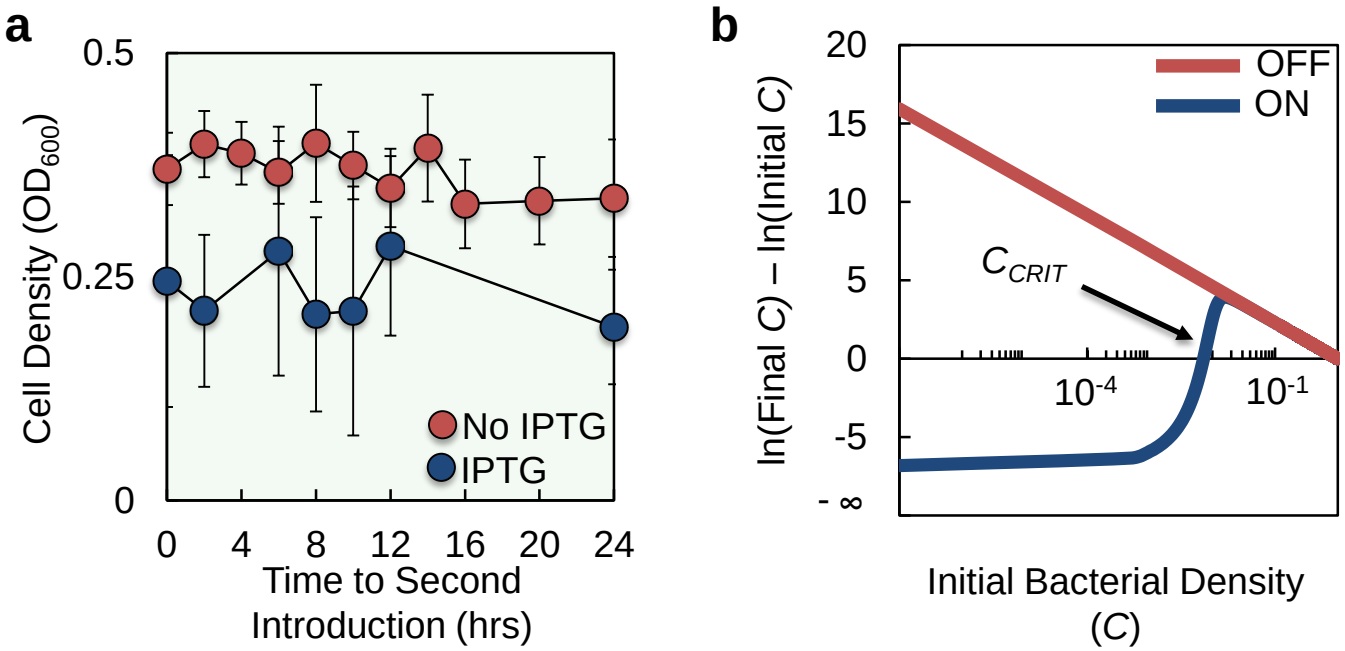
a
0.5
0.25
0
Cell Density (OD600)
0
4
8
12
16
20
24
Time to Second Introduction (hrs)
No IPTG
IPTG
b
20
15
10
5
0
-5
- ∞
ln(Final C) – ln(Initial C)
OFF
ON
CCRIT
10-4
10-1
Initial Bacterial Density (C)

figure S6

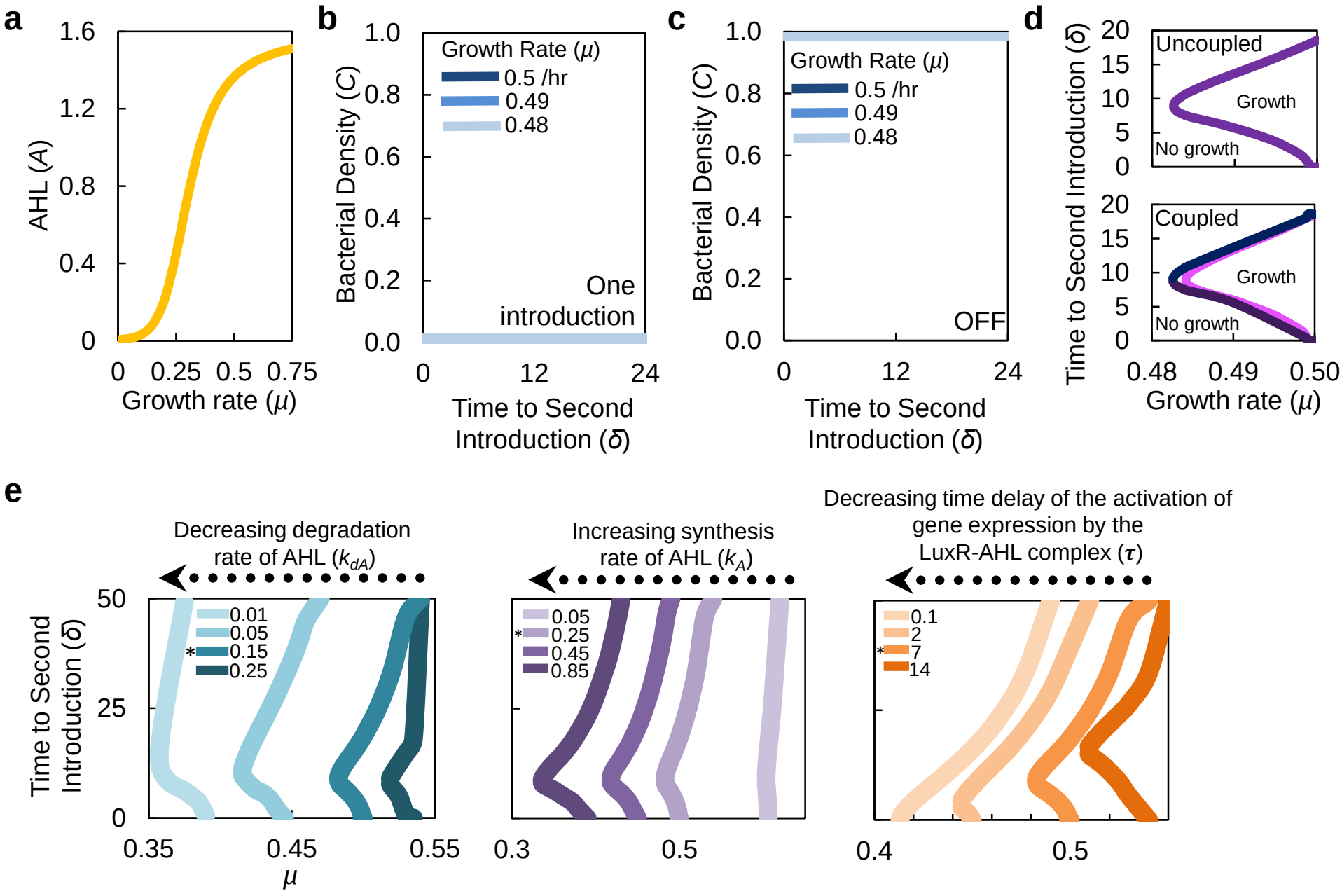
a
AHL (A)
Growth rate (μ)
b
Bacterial Density (C)
Growth Rate (μ)
0.5 /hr
0.49
0.48
One introduction
Time to Second Introduction (δ)
c
Bacterial Density (C)
Growth Rate (μ)
0.5 /hr
0.49
0.48
OFF
Time to Second Introduction (δ)
d
Time to Second Introduction (δ)
Uncoupled
Growth
No growth
Coupled
Growth
No growth
Growth rate (μ)
e
Decreasing degradation rate of AHL (k_{dA})
0.01
0.05
*0.15
0.25
Increasing synthesis rate of AHL (k_A)
0.05
*0.25
0.45
0.85
Decreasing time delay of the activation of gene expression by the LuxR-AHL complex (τ)
0.1
2
*7
14
Time to Second Introduction (δ)
μ

figure S7

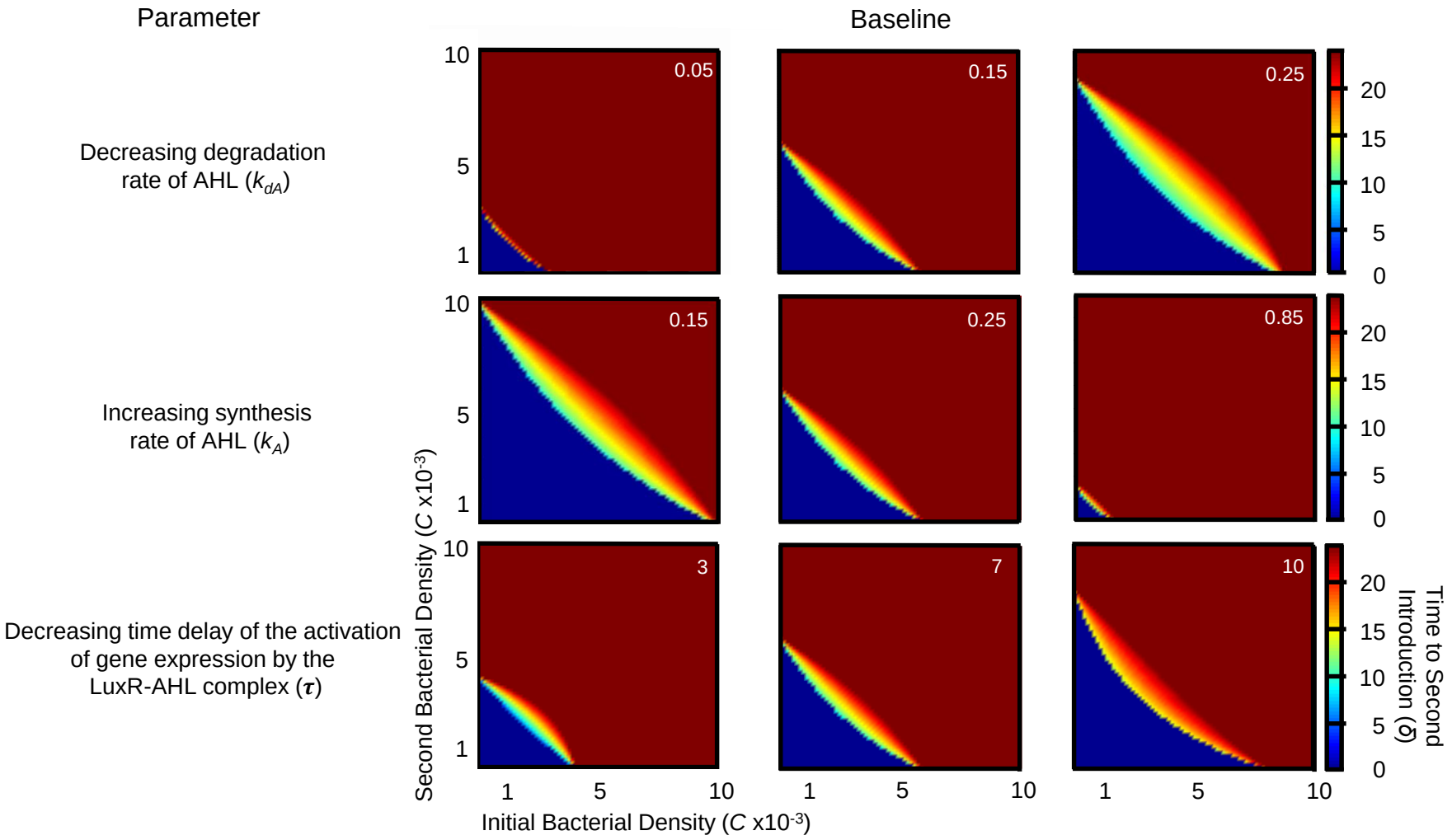
Parameter
Baseline
Decreasing degradation rate of AHL (k_{dA})
Increasing synthesis rate of AHL (k_A)
Decreasing time delay of the activation of gene expression by the LuxR-AHL complex (τ)
0.05
0.15
0.25
0.15
0.25
0.85
3
7
10
Second Bacterial Density (C x10^{-3})
Initial Bacterial Density (C x10^{-3})
Time to Second Introduction (δ)
1
5
10
0
15
20

figure S8

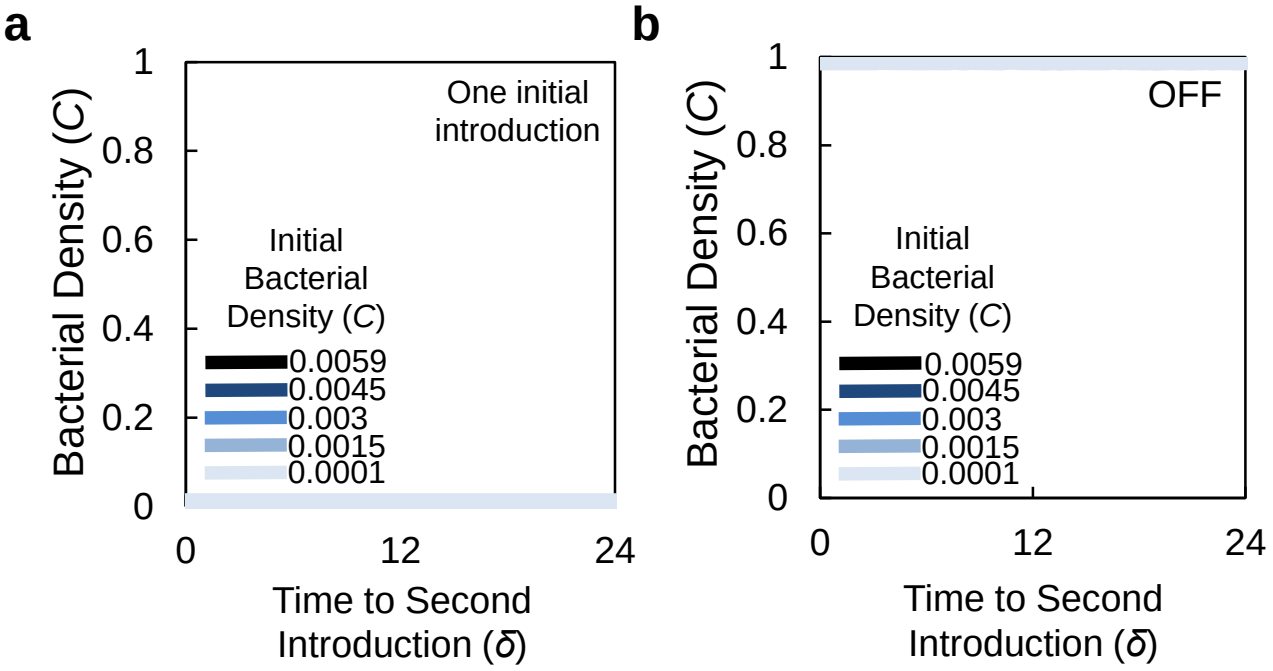
a
b
Bacterial Density (C)
Time to Second Introduction (δ)
One initial introduction
OFF
Initial Bacterial Density (C)
0.0059
0.0045
0.003
0.0015
0.0001
0
0.2
0.4
0.6
0.8
1
0
12
24

figure S9

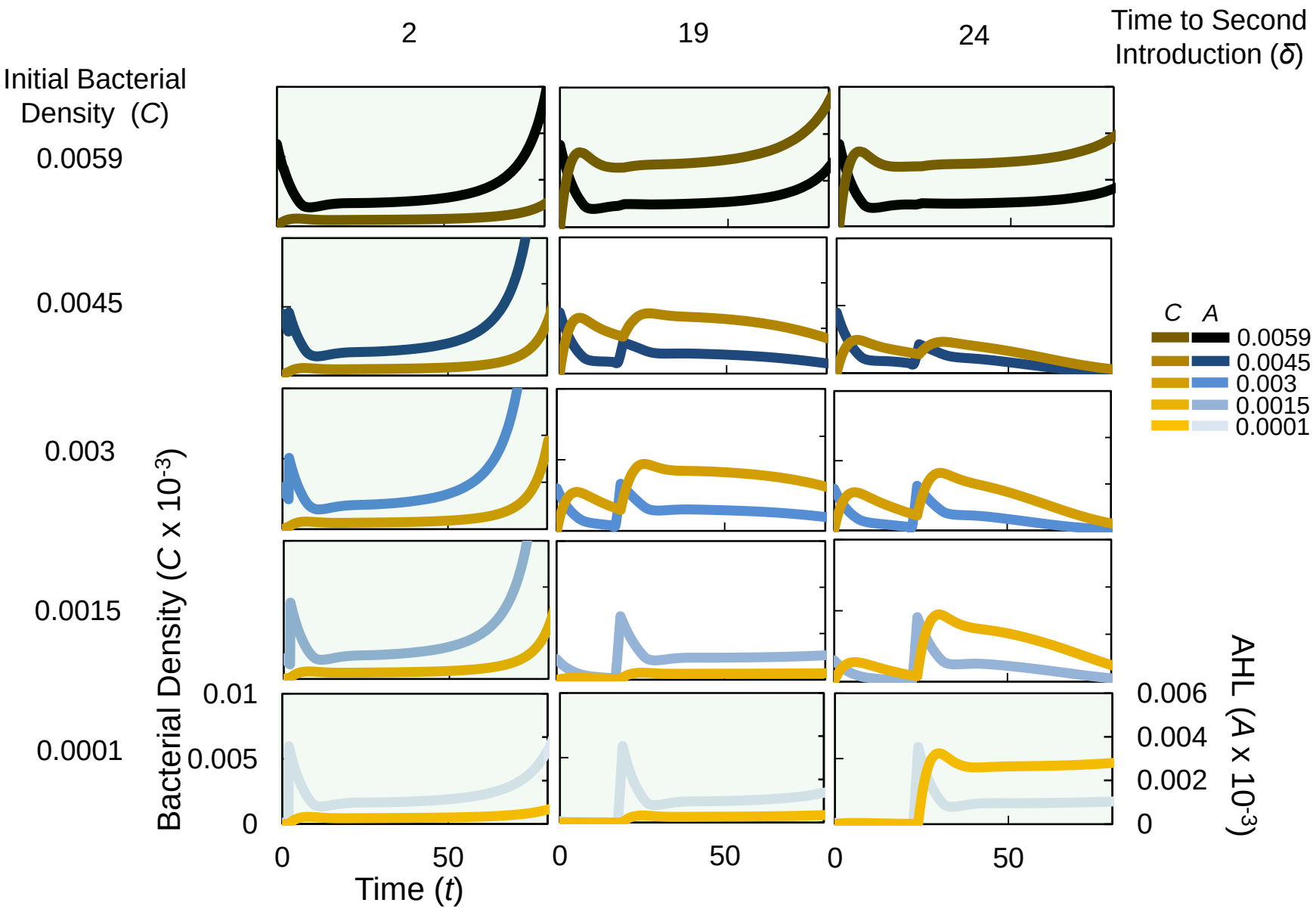
Time to Second Introduction (δ)
2
19
24
Initial Bacterial Density (C)
0.0059
0.0045
0.003
0.0015
0.0001
C A
0.0059
0.0045
0.003
0.0015
0.0001
Bacterial Density (C x 10-3)
0.01
0.005
0
AHL (A x 10-3)
0.006
0.004
0.002
0
0
50
Time (t)